Realization of Microlens Array on Flat Encapsulant Layer for Enhancing Light Efficiency of COB-LEDs

Xingjian Yu, Linyi Xiang, Shuling Zhou, Naiqi Pei, and Xiaobing Luo, *Fellow, IEEE*

***Abstract*— The conventional chip-on-board light-emitting diodes (COB-LEDs) with flat encapsulant layer present low light efficiency due to the total internal reflection (TIR) happens at the encapsulant-air interface. In this study, microlens array was realized on the flat encapsulant layer of COB-LEDs to diminish the TIR at the encapsulant-air interface. The microlens array was fabricated by selectively exposing the UV glue film in UV-light through a pre-designed photomask. Micro-pillars form after the UV-light exposure and microlens array forms spontaneously due to the wetting process of uncured UV glue on the micro-pillars. The geometry of the microlens array was experimentally optimized, and the light efficiency enhancement of COB-LEDs by the microlens array was analyzed. The results show that optimal geometry of microlens array with curvature of ∼41° and base diameter of ∼87 μm can be realized by adjusting the UV-light exposure time as >40 s and UV glue film thickness as >80 μm. Compared to the traditional flat encapsulant layer, the microlens array with optimal geometry increases the light efficiency of blue and ∼5000 K white COB-LEDs by 50.9% and 9.31%.**

***Index Terms*— Chip-on-board light-emitting diodes, microlens array, total internal reflection, light efficiency.**

I. Introduction

WHITE light-emitting diodes (LEDs) have many advantages over the conventional light sources, and have been the mainstream light source in 21st century[1]. In white LED packaging, the phosphor/silicone encapsulant layer plays an important role in light conversion, correlated color temperature (CCT) manipulation and oxygen/moisture protection [2]–[4]. However, serious total internal reflection (TIR) happens at the chip-encapsulant and encapsulant-air interfaces due to the refractive index difference of LED chip (∼2.5), encapsulant (1.4∼1.7) and air (=1), which decreases the light efficiency of LEDs significantly.

In the past decades, microlens arrays [5]–[13] were fabricated on the LED chips by photolithography [5]–[8] and nano-microspheres deposition [12], [13] to diminish the TIR at the chip-encapsulant interface. However, the TIR at the encapsulant-air interface was rarely studied because most of the previous studies are focus on the design of single chip LEDs. For single chip LEDs shown in Fig. 1(a), an overall hemispherical lens is fasten above the encapsulant layer to guide the light to emit out from the encapsulant-air interface directly. Therefore, the TIR at the encapsulant-air interface of single chip LEDs can be ignored. However, with the increasing packaging demand of high power and compact size, the single chip LEDs no longer meet the requirement. Under this background, the chip-on-board LEDs (COB-LEDs) with dozens to hundreds of LED chips shown as Fig. 1(b) are becoming more and more popular in recent years. Compared to the single chip LEDs, the size of the COB-LEDs with same output power can be reduced by dozen times. However, the substrate area of COB-LEDs is dozen times of that of the single chip LEDs. Therefore, it is impossible to use overall lens in COB-LEDs packaging because it consumes too much silicone to fill in the encapsulant-lens gap and increases the module's size significantly. As a results, the commercial COB-LEDs present flat encapsluant-air interface shown as Fig. 1(b), which induces serious TIR with critical incident angles of $\theta_c < 46°$ due to the refractive index difference of the encapsulant and air [14]–[18].

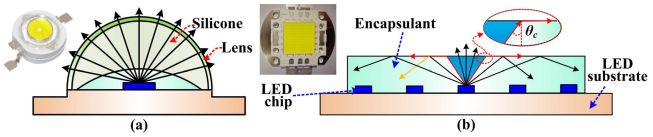

Fig. 1. Schematic diagram of the light propagation in (a) single chip LEDs with overall hemispherical lens and (b) COB-LEDs with flat encapsulant layer.

Few methods were proposed to diminish the TIR at encapsulant-air interface of COB-LEDs, including introducing patterned substrate [14], using scattering materials [15] and designing dome-shaped encapsulant layer [16]–[18]. These methods enhance the light efficiency of blue and white COB-LEDs by >40% and >10%. Besides, the dome-shaped encapsulant layers were proved to have higher light efficiency enhancement than other methods because it guides the light to emit out from the encapsulant-air interface directly. However, the reported dome-shaped encapsulant layers with millimeter size are only suitable for COB-LEDs with sparse chip distribution in row or column. Therefore, more works needs to be done to solve the TIR at encapsulant-air interface for COB-LEDs with dense chip distribution.

Manuscript received June 20, 2020; revised August 27, 2020; accepted September 3, 2020. Date of publication September 8, 2020; date of current version September 18, 2020. This work was supported in part by the National Natural Science Foundation of China under Grant 51625601, in part by the China Postdoctoral Science Foundation under Grant 2020M672346, in part by the Ministry of Science and Technology of the People's Republic of China under Grant 2017YFE0100600, in part by the Creative Research Groups Funding of Hubei Province under Grant 2018CFA001, in part by the Open Project Program of Wuhan National Laboratory for Optoelectronics under Grant 2018WNLOKF017, and in part by the Postdoctoral Creative Research Funding of Hubei Province. *(Corresponding author: Xiaobing Luo.)*

The authors are with the School of Energy and Power Engineering, Huazhong University of Science and Technology, Wuhan 430074, China (e-mail: luoxb@mail.hust.edu.cn).

Color versions of one or more of the figures in this letter are available online at http://ieeexplore.ieee.org.

Digital Object Identifier 10.1109/LPT.2020.3022794

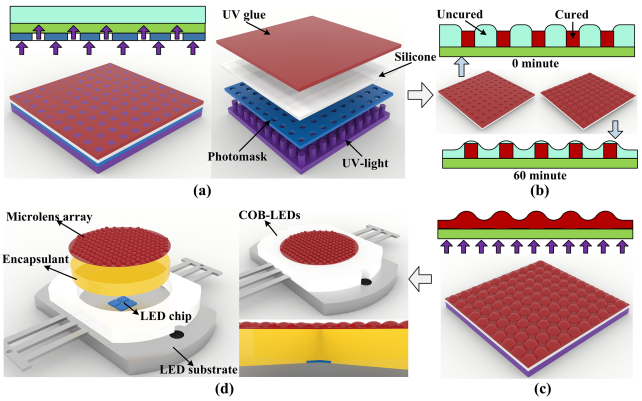

Fig. 2. Fabrication process of microlens array and its application in COB-LEDs packaging. (a) exposing UV glue film in UV-light through a photomask for 60 s, (b) removing the photomask for 60 minutes, (c) exposing the whole UV glue film in the UV-light for 60 s, (d) integrating the silicone film with microlens array on the encapsulant layer of the COB-LEDs.

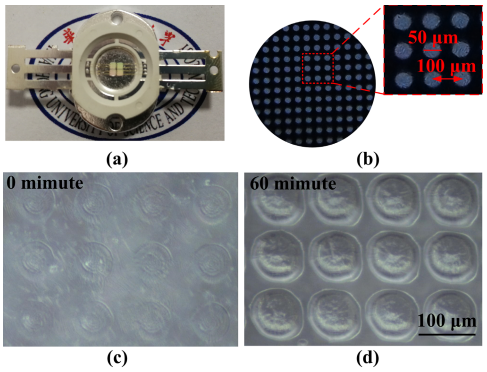

Fig. 3. Images of (a) structure of the COB-LEDs, (b) photomask, (c) geometry of the UV glue film when the UV-light was just removed and (d) geometry of the microlens array after removing the UV-light for 60 minutes.

Inspired by the prior works of microlens array on the LED chip, it seems that fabricating microlens array on the encapsulant layer might be a good way to increase the light efficiency of COB-LEDs with dense chip distribution. However, the photolithography and nano-microspheres deposition methods are not suitable for realizing lens array on the encapsulant layer due to the complicated wetting and curing behaviors of the encapsulant [19]. Recently, *Zhou* and *Ren* proposed an method to realize microlens array on the glass substrate[20] by selectively curing photosensitive monomer material, which could be an alternative method for realizing microlens array on the encapsulant layer.

In this study, a simple method [20] was applied to realize microlens array on the encapsulant layer for enhancing the light efficiency of COB-LEDs. Compared with the previous methods [16]–[18], this method is simpler and independent on the structure and chip distribution of COB-LEDs. The forming mechanism of the microlens array was verified, and the geometry of microlens array was experimentally optimized. The light efficiency enhancement of COB-LEDs by the microlens arrays were measured and analyzed.

II. Experimrents

Fig. 2 shows the fabrication process of the microlens array and its application in COB-LEDs packaging, it consists of the following steps.

a) Preparing a thin silicone film (OE6550A/B, Dow corning) with thickness of ∼100 μm and coating a thin layer of transparent UV glue (9308, Leaftop) on the silicone film. The thickness of the silicone and UV glue film is adjusted by a coating machine (Weida, AFA-V). Attaching a photomask with transparent circular pattern on the silicone film and exposing the UV glue film to a collimated UV-light with wavelength of 365 nm and intensity of 15 mW/cm^2 for 60 s. Attribute to the presence of the photomask, the UV glue that exposed to the UV-light cures (polymerized) to form micro-pillars [20].

b) Removing the UV-light and photomask for 60 minutes. When the UV-light was just removed, the UV glue film has shallow pits at the position of pillars due to the volume shrink of the UV glue at the polymerization process [20], [21]. Then the uncured UV glue wets the cured pillars gradually driven by the capillary force and forms microlens array spontaneously.

c) Exposing the whole UV glue film to the UV-light for 60 s to cure it and silicone film with microlens array is obtained.

d) Integrating the silicone film with microlens array on the encapsulant layer of COB-LEDs.

In the experiments, blue and ∼5000 K white COB-LEDs with and without microlens array were prepared, and their light efficiency was measured by an integrating sphere (ATA-1000, Everfine). For blue LEDs, silicone (OE6550A/B, Dow corning) was used as the encapsulant. For white COB-LEDs, yellow phosphor (YAG-O4, Intematix) was mixed with the silicone with mass concentration of 0.04 g: 1 g to form the encapsulant. The thickness of the encapsulant was kept as ∼1 mm.

III. Results and Discussion

Fig. 3(a) shows the structure of the COB-LEDs used in the experiments. 4 conventional chips with size of 1 mm×1 mm are arranged closely with chip spacing of 1.2 mm. Fig. 3(b) shows the photomask used in the experiments, the diameter and spacing of the transparent circular pattern are 50 μm and 100 μm. Fig. 3(c) shows the geometry of the UV glue film when the UV-light was just removed, shallow pits were observed on the film. Fig. 3(d) shows the geometry of the UV glue film after removing the UV-light for 60 minutes, microlens array was observed on the film.

Fig. 4 shows the geometry of microlens arrays that realized with UV glue thickness of 50 μm, 100 μm and 200 μm. It shows microlens array was only achieved at thickness of 50 μm and 100 μm. Besides, the curvature of microlens θ with UV glue thickness of 50 μm and 100 μm are ∼32° and ∼41°, and the base diameter of the microlens D with UV glue thickness of 50 μm and 100 μm are ∼70 μm and ∼87 μm. The height of the pillar is assumed to be the main reason for inducing the geometry difference of the microlens arrays. To verify this assumption, the uncured UV

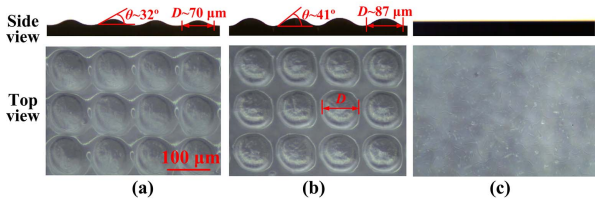

Fig. 4. Geometry of microlens arrays with UV glue thickness of (a) 50 μm, (b) 100 μm and (c) 200 μm.

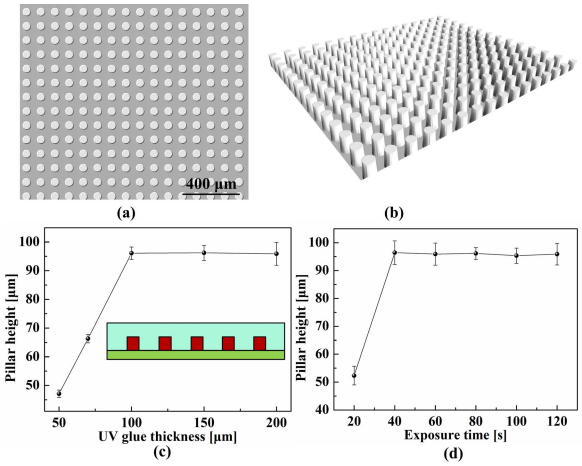

Fig. 5. Characterization of pillar geometry after first UV-light exposure. (a) pillar geometry from top view, (b) pillar geometry from oblique view, (c) pillar height at various UV glue thickness, (d) pillar height at various exposure time.

glue was washed away after the first UV-light exposure and the geometry of the pillars was characterized by microscope, the results are shown in Fig. 5. Fig. 5(a) and Fig. 5(b) show the geometry of the pillars at UV glue thickness of ~100 μm. It shows that pillar array forms after first UV-light exposure and the height of the pillars was measured ~95 μm. The height of the pillars is slightly smaller than the thickness of UV glue due to the volume shrink of the UV glue at the polymerization process [20], [21]. Fig. 5(c) shows the pillar height under UV glue thickness of 50 μm to 200 μm, when the exposure time was set as 60 s. It shows that the pillar height rarely changes when the UV glue thickness is larger than 100 μm, which indicates that ~100 μm might be the maximum curing depth of the UV glue by the UV-light source used in the experiments. Therefore, we measured the pillar height under exposure time of 20 s to 120 s, when the UV glue thickness was set as 200 μm. Fig. 5(d) indicates that the pillar height rarely changes when the exposure time is larger than 40 s, which indicates that the maximum curing depth by the UV-light source is ~100 μm. This is because the intensity of UV light decreases with its transmission depth in the UV glue film, and it drops below the critical exposure intensity of the UV glue at transmission depth of >100 μm. As a result, the UV glue at thickness of >100 μm cannot be cured by the UV-light source even increases the exposure time.

For UV glue thickness of 50 μm and 100 μm, the pillars penetrate the entire film and microlens array forms at the top

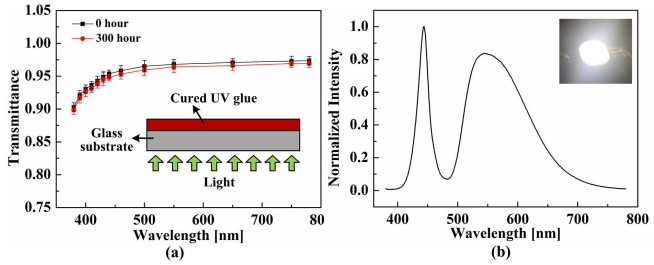

Fig. 6. Reliability verification of UV glue. (a) Transmittance of UV glue before and after exposing in white light for 300 hours, (b) spectra of ~5000 K phosphor-converted white LED.

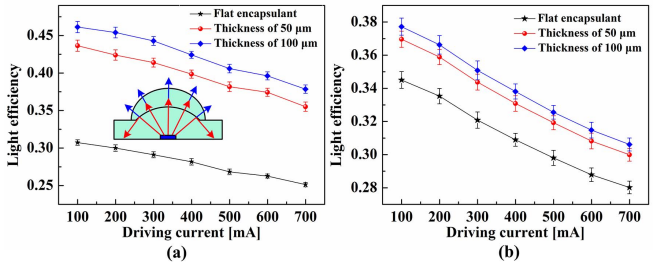

Fig. 7. Light efficiency of COB-LEDs with flat encapsulant layer and with microlens arrays shown in Fig. 4(a) and Fig. 4(b). (a) Blue COB-LEDs, (b) ~5000 K white COB-LEDs.

surface of the film. Because the pillar height at thickness of 100 μm is higher than that of 50 μm, so the curvature and base diameter of the microlens at thickness of 100 μm are larger than that of 50 μm due to the stronger capillary effect. However, for UV glue thickness of 200 μm, it fails to form microlens array because the pillars are fully immersed in the uncured UV glue shown as the insert figure of Fig. 5(c).

The microlens arrays were integrated on the encapsulant layer of COB-LEDs to improve their light efficiency. Firstly, experiments were conducted to confirm whether the reliability of the UV glue is satisfied if it directly used as microlens. As shown in the insert figure of Fig. 6(a), a 1mm glass substrate with ~100 μm cured UV glue film was exposed to white LED light with light spectra shown in Fig. 6(b) for 300 hours, and the transmittance of the UV glue before and after white light exposing is shown in Fig. 6(a). The transmittance of UV glue is defined as the transmittance ratio of the coated substrate to the uncoated substrate. It shows that the UV glue presents high transmittance at wavelength >400 nm, which proves its apply feasibility on LED packaging because the intensity of the while LEDs spectra is mainly distributed at wavelength of >400 nm shown as Fig. 6(b). In addition, the transmittance of UV glue rarely changes after exposing in white LED light for 300 hours, which indicates that the reliability of UV glue is satisfied if it directly used as microlens in LED packaging.

Fig. 7 shows the light efficiency of blue and ~5000 K white COB-LEDs with flat encapsulant layer and microlens arrays shown in Fig. 4(a) and Fig. 4(b) at driving current of 100 mA to 700 mA. Compared with the flat encapsulant, the microlens arrays shown in Fig. 4(a) and Fig. 4(b) enhance the

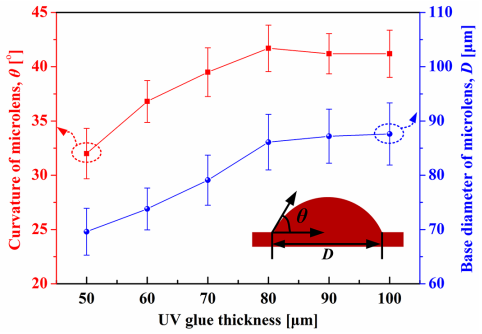

Fig. 8. Curvature and base diameter of microlens at various UV glue thickness.

light efficiency of blue COB-LEDs by 41.9% and 50.9%, and enhance the light efficiency of ~5000 K white COB-LEDs by 7.09% and 9.31%. The light efficiency enhancement is measured as the average light efficiency enhancement at different driving currents. And the light efficiency enhancement at each driving current is defined as $(\eta_{lens}\text{-}\eta_{flat})/\eta_{flat} \times 100\%$, where η_{lens} is the light efficiency of COB-LEDs with microlens array and η_{flat} is the light efficiency of COB-LEDs without microlens array (with flat encapsulant layer). As the insert figure of Fig. 7(a) shows, more light can emit out from the microlens-air interface for microlens array with higher curvature and larger base diameter. Therefore, the light efficiency of COB-LEDs with microlens array shown in Fig. 4(b) is higher than that with microlens array shown in Fig. 4(a).

The results shown in Fig. 7 indicate that the light efficiency enhancement of COB-LEDs by the microlens array depends on the curvature and base diameter of the microlens, while the results in Fig. 4 show the curvature and base diameter of microlens depends on the UV glue thickness. Therefore, more experiments were conducted to investigated the dependence of the curvature/base diameter of microlens and UV glue thickness, and the results are shown in Fig. 8. It can be seen that the curvature and base diameter of microlens increase with the UV glue thickness initially and rarely change when the UV glue thickness is larger than 80 μm. Therefore, the geometry of microlens array shown in Fig. 4(b) is optimal in this study.

IV. Conclusion

In this study, microlens arrays were realized and applied to the COB-LEDs packaging. The forming mechanism of the microlens array was verified, and the geometry of the microlens was experimentally optimized by adjusting the UV-light exposure time and the UV glue thickness. The light efficiency of the COB-LEDs with and without microlens array was measured and analyzed. The results show that micro-pillars form after the first UV-light exposure, and microlens array forms spontaneously due to the wetting process of the uncured UV glue on the pillars. The geometry of the microlens array depends on the pillar height. A maximum pillar height was achieved at UV glue thickness of >100 μm and exposure time of >40 s, and optimal geometry of microlens array with curvature of ~41° and base diameter of ~87 μm was achieved at pillar height of >80 μm. Compared to the flat encapsulant layer, the microlens array with optimal geometry increases the light efficiency of blue and ~5000 K white COB-LEDs by 50.9% and 9.31%.

References

[1] X. Luo, R. Hu, S. Liu, and K. Wang, "Heat and fluid flow in high-power LED packaging and applications," *Prog. Energy Combustion Sci.*, vol. 56, pp. 1–32, Sep. 2016.
[2] X. Yu, W. Shu, R. Hu, B. Xie, Y. Ma, and X. Luo, "Dynamic phosphor sedimentation effect on the optical performance of white LEDs," *IEEE Photon. Technol. Lett.*, vol. 29, no. 14, pp. 1195–1198, Jul. 15, 2017.
[3] X. Yu, B. Xie, Q. Chen, Y. Ma, R. Wu, and X. Luo, "Thermal remote phosphor coating for phosphor-converted white-light-emitting diodes," *IEEE Trans. Compon., Packag., Manuf. Technol.*, vol. 5, no. 9, pp. 1253–1257, Sep. 2015.
[4] R. Hu *et al.*, "Near-/mid-field effect of color mixing for single phosphor-converted light-emitting diode package," *IEEE Photon. Technol. Lett.*, vol. 25, no. 3, pp. 246–249, Feb. 2013.
[5] D. Kim, H. Lee, N. Cho, Y. Sung, and G. Yeom, "Effect of GaN microlens array on efficiency of GaN-based blue-light-emitting diodes," *Jpn. J. Appl. Phys.*, vol. 44, nos. 1–7, pp. 42–45, 2005.
[6] H. W. Choi *et al.*, "GaN micro-light-emitting diode arrays with monolithically integrated sapphire microlenses," *Appl. Phys. Lett.*, vol. 84, no. 13, pp. 2253–2255, Mar. 2004.
[7] M. Khizar, Z. Y. Fan, K. H. Kim, J. Y. Lin, and H. X. Jiang, "Nitride deep-ultraviolet light-emitting diodes with microlens array," *Appl. Phys. Lett.*, vol. 86, no. 17, pp. 1–3, 2005.
[8] R. Liang *et al.*, "High light extraction efficiency of deep ultraviolet LEDs enhanced using nanolens arrays," *IEEE Trans. Electron Devices*, vol. 65, no. 6, pp. 2498–2503, Jun. 2018.
[9] Y. Qu, J. Kim, C. Coburn, and S. R. Forrest, "Efficient, nonintrusive outcoupling in organic light emitting devices using embedded microlens arrays," *ACS Photon.*, vol. 5, no. 6, pp. 2453–2458, Jun. 2018.
[10] F. Galeotti, W. Mróz, G. Scavia, and C. Botta, "Microlens arrays for light extraction enhancement in organic light-emitting diodes: A facile approach," *Organic Electron.*, vol. 14, no. 1, pp. 212–218, Jan. 2013.
[11] E. Wrzesniewski *et al.*, "Enhancing light extraction in top-emitting organic light-emitting devices using molded transparent polymer microlens arrays," *Small*, vol. 8, no. 17, pp. 2647–2651, Sep. 2012.
[12] Z. Zhu *et al.*, "Improvement of light extraction of LYSO scintillator by using a combination of self-assembly of nanospheres and atomic layer deposition," *Opt. Express*, vol. 23, no. 6, p. 7085, 2015.
[13] J. Y. Park, G. S. Rama Raju, B. K. Moon, and J. H. Jeong, "Facile solvothermal synthesis of high refractive index ZrO_2 spheres: Estimation of the enhanced light extraction efficiency," *RSC Adv.*, vol. 5, no. 100, pp. 81915–81919, 2015.
[14] Z.-T. Li, Q.-H. Wang, Y. Tang, C. Li, X.-R. Ding, and Z.-H. He, "Light extraction improvement for LED COB devices by introducing a patterned leadframe substrate configuration," *IEEE Trans. Electron Devices*, vol. 60, no. 4, pp. 1397–1403, Apr. 2013.
[15] H. Zheng, L. Li, X. Lei, X. Yu, S. Liu, and X. Luo, "Optical performance enhancement for Chip-on-Board packaging LEDs by adding TiO_2/silicone encapsulation layer," *IEEE Electron Device Lett.*, vol. 35, no. 10, pp. 1046–1048, Oct. 2014.
[16] X. Yu, B. Xie, B. Shang, W. Shu, and X. Luo, "A facile approach to fabricate patterned surfaces for enhancing light efficiency of COB-LEDs," *IEEE Trans. Electron Devices*, vol. 64, no. 10, pp. 4149–4155, Oct. 2017.
[17] X. Yu, R. Hu, R. Wu, B. Xie, X. Zhang, and X. Luo, "Cylindrical tuber encapsulant layer realization by patterned surface for chip-on-board light-emitting diodes packaging," *J. Electron. Packag.*, vol. 141, no. 3, pp. 1–5, Sep. 2019.
[18] X. Yu, B. Xie, B. Shang, Q. Chen, and X. Luo, "A cylindrical tuber encapsulant geometry for enhancing optical performance of chip-on-board packaging light-emitting diodes," *IEEE Photon. J.*, vol. 8, no. 3, pp. 1–9, Jun. 2016.
[19] X. J. Yu, R. Hu, L. L. Zhou, H. Wu, and X. B. Luo, "Spreading and curing behaviors of a thermosetting droplet-silicone on a heated surface," *J. Harbin Inst. Technol.*, vol. 26, no. 4, pp. 1–8, 2019.
[20] Z. Zhou and H. Ren, "Polymeric microlens array formed directly on glass plate," *Opt. Eng.*, vol. 56, no. 1, Jan. 2017, Art. no. 015106.
[21] X. Yang *et al.*, "Fabrication of UV-curable solvent-free epoxy modified silicone resin coating with high transparency and low volume shrinkage," *Prog. Organic Coat.*, vol. 129, pp. 96–100, Apr. 2019.